6

Alterations in the Brainstem Preautonomic Circuitry May Contribute to Hypertension Associated with Metabolic Syndrome

Bradley J. Buck[1], Lauren K. Nolen[2], Lauren G. Koch[3], Steven L. Britton[4] and Ilan A. Kerman[5]
[1]*College of Medicine, The University of Toledo, OH,*
[2] *Genetics and Genomic Sciences Theme, Graduate Biomedical Sciences Program, University of Alabama at Birmingham, AL,*
[3]*Department of Anesthesiology, University of Michigan,*
[4]*Department of Physical Medicine and Rehabilitation, University of Michigan,*
[5]*Department of Psychiatry and Behavioral Neurobiology, University of Alabama at Birmingham, AL,*
USA

1. Introduction

Metabolic syndrome (MetS) is defined as a co-occurrence of insulin resistance, obesity (specifically visceral adipose tissue accumulation), hypertriglyceridemia, and hypertension (HTN) (Grundy et al., 2004; Fig. 1). MetS has been implicated in the development of atherosclerosis, heart disease, type-2 diabetes, and has significantly contributed to morbidity and mortality around the world (Rizzo et al., 2006; Lorenzo et al., 2006). The number of people living with MetS in the United States has steadily increased in recent years. It was estimated that in the year 2000 over 47 million Americans had MetS (Ford et al., 2002), while in 2005 that number increased to 50 million (Alberti et al., 2005). Due to the serious consequences of the above conditions, timely research is needed to discover and understand the underlying pathophysiology of this illness.

1.1 Genetic basis of metabolic syndrome

Recent evidence indicates a complex genetic background for MetS. Rather than being defined by specific mutations in a small number of genes, it is best described as a cluster of genetic traits that differs from patient to patient. Many studies have reported associations between various single nucleotide polymorphisms (SNPs) and individual defining traits of MetS; however, none of these studies has been able to extend that association to the disease as a whole. For instance, a genome wide association study (GWAS) of Indian Asian men by Zabaneh and Balding (2010) found numerous SNPs that were significantly associated with metabolic traits such as high HDL-cholesterol, type-2 diabetes, and increased diastolic blood pressure, but none were also associated with the overall MetS phenotype. In a similar study, Wong et al. (2007) described a polymorphism in the gene for human melanocortin receptor

3, which was significantly associated with insulin resistance in the Maori kindred but did not predict the syndrome as a whole.

Diagnostic criteria for Metabolic Syndrome

Central obesity

- BMI >30 kg/m^2

Plus any two of the following:

Raised triglycerides

- >150 mg/dL
- Treatment for this lipid abnormality

Reduced HDL-cholesterol

- <40 mg/dL in men
- <50 mg/dL in women
- Treatment for this lipid abnormality

Raised blood pressure

- Systolic ≥130 mm Hg
- Diastolic ≥85 mm Hg
- Medicinal treatment for hypertension

Raised fasting plasma glucose

- Fasting plasma glucose ≥100 mg/dL
- Type 2 diabetes

*Adapted from Alberti et al., 2005.

Fig. 1. Diagnostic criteria for metabolic syndrome as proposed by the International Diabetes Federation. Abbreviations: BMI, body mass index – weight (kg) divided by the square of the height (m).

One possible reason for past struggles, as reported by Mei et al. (2010), is the phenomenon of gene pleiotropy, or the instance of one gene affecting multiple phenotypes. In the case of single-trait association studies, gene pleiotropy may cause a loss of statistical power and thus the ability to find significant effects. Using a computational model that accounts for such effects, Mei et al. (2010) were able to identify eleven gene variants that were significantly associated with MetS. Several of these genes had even been previously associated with individual metabolic traits, but had failed to be significantly correlated with

the syndrome itself. Even without advanced computational methods, some investigators have reported certain genotypes that predict the development of MetS.

For example, Leu et al. (2011) reported an adiponectin gene variant that was significantly correlated with MetS as well as the development of hypertension, and Devaney et al. (2011), found that the H1 haplotype of the *akt1* gene was strongly associated with metabolic syndrome in a population of African-American and European-American subjects. Taken together, recent data indicate a strong, yet evolving, genetic component to MetS. This evidence yields support for using selectively-bred animal strains as appropriate models for the disease.

1.2 Animal models of metabolic syndrome

In the past several decades, multiple animal models of MetS have been proposed, most of them in rats (see review by Artinano and Castro, 2009). Currently, obese Zucker rats are the most commonly used model. These rats exhibit many of the features of MetS, including obesity, dyslipidaemia, insulin resistance, and hypertension (Zucker and Zucker, 1961). While these phenotypes represent the key components of MetS in humans, one major drawback of the obese Zucker model is its reliance on disruption of the leptin receptor gene, which does not reflect the genetic background of the disease in humans (Chua et al., 1996). Several strains of spontaneously hypertensive rats (SHRs) have also been used to model MetS, but suffer the drawback of the same genetic basis as the obese Zucker rats (Ishizuka et al., 1998).

A more realistic model was developed in 2007 by Kovacs et al. The Wistar Ottawa Karlsburg W (WOKW) rats, like other models, exhibit the key features of MetS but have a polygenic background that makes the model more applicable to human disease (Kovacs et al., 2000). Recently, the WOKW rats have been used to identify quantitative trait loci for several of the major traits of MetS, as well as to establish an association between MetS and impaired coronary function (Grisk et al., 2007).

Recently a new animal model of MetS was developed. Selective breeding of a population of rats based on their intrinsic running capacity produced rats exhibiting physiological characteristics similar to those seen in metabolic syndrome. Low capacity runners (LCRs), those rats unable to run extensive distances, exhibited, compared to their high capacity runner counterparts (HCRs), elevated fasting glucose levels, triglyceride levels, free fatty acid levels, visceral adipose tissue accumulation, and blood pressure (Wisloff et al., 2005). Additionally, elevated levels of insulin were also discovered in LCRs, while the difference in c-peptide levels, the peptide sequence released when proinsulin is cleaved to insulin and c-peptide, between HCRs and LCRs was not significant. These data implicate insulin resistance in the LCRs, as exhibited by the decrease in insulin clearance (the ratio between measured insulin and c-peptide). Taken together, these data by Wisloff et al. (2005) suggest that the LCR rat may be used as a model of MetS.

The goal of the current study is to investigate possible brainstem neural mechanisms of hypertension associated with MetS in the LCR model. Previous work has documented a 13.2% increase in the 24-hour mean arterial pressure (MAP) in the LCR rats as compared to their HCR counterparts (Wisloff et al. 2005).

1.3 Brainstem cardiovascular circuitry

Brainstem regulation of vascular tone is a delicate balance between excitatory and inhibitory influences. To understand and appreciate this pathway we provide the reader with: (1) the major transmitters within the circuit; (2) the discrete brainstem nuclei involved in the circuit; and (3) the interplay between the nuclei resulting in altered vascular tone. We begin here with a discussion of the main neurotransmitters, followed by a review of the involved nuclei and their circuitry.

1.3.1 Neurotransmitters

Brainstem cardiovascular circuitry overwhelmingly involves but two transmitters: γ-aminobutyric acid (GABA) and glutamate (Talman et al, 1980; Andersen et al., 2001; Suzuki et al., 1996; Gordon & Sved, 2002; Minson et al., 1997).

GABA is synthesized intra-cellularly from glutamate in a decarboxylation reaction guided by the enzyme glutamic acid decarboxylase, or GAD. Interestingly, GAD has two isoforms, or variants, coded for on separate chromosomes. These are referred to GAD65 and GAD67, with the numbers representing their atomic mass in kilodaltons. While the significance of having two isoforms is yet to be determined, some believe GAD65 is responsible for local control of GABA synthesis while GAD67 is responsible for long-term maintenance of baseline GABA levels within neural tissue (Esclapez et al., 1994; Esclapez & Houser, 1999). Additionally, it is generally believed the two isoforms are localized within different cellular compartments. GAD67 is associated predominantly with cytoplasmic pools of GABA, while GAD65 is associated with vesicular pools of GABA (Soghomonian & Martin, 1998). Thus, it is likely that GAD67 regulates GABA synthesis for metabolic functions of the cell, while GAD65 regulates GABA synthesis for synaptic release (Soghomonian & Martin, 1998).

Glutamate, conversely, is predominantly derived from extra-cellular stores and concentrated in neural tissue via cytoplasmic transporters (Danbolt, 2001; Kang et al., 2001). For this reason, quantification is much more difficult and includes, at the very least, expression analysis of glutamate transporters, and more accurately, direct sampling of synaptic cleft concentrations.

1.3.2 Neural control of cardiovascular function

Within the last 20 years a number of investigators have used expression of the immediate early gene, c-fos, as a marker of baro-sensitive neurons following alterations in blood pressure. In such studies hyper- or hypo- tension was experimentally induced by administration of specific vasoactive drugs (e.g. phenylephrine to increase blood pressure). These studies have pointed to three main brain regions being involved in cardiovascular regulation: the nucleus tractus solitarius (NTS), the caudal ventrolateral medulla (CVLM), and the rostral ventrolateral medulla (RVLM) (Chan and Sawchenko, 1994; Graham et al., 1995; Miura, 1994). Phenotyping of these barosensitive neurons demonstrates an intricate relay of information between these nuclei resulting in end organ modulation.

The brainstem cardiovascular network begins in the stretch sensitive baroreceptors of the carotid sinus and aortic arch. It is here that afferent signals are produced. Traveling via the glossopharyngeal and vagus nerves, the signal is relayed to caudal NTS neurons of the medulla (Spyer, 1994). These afferent projections are likely glutamatergic (Talman et al,

1980; Andersen et al., 2001). And while the NTS contains heterogeneous neuronal populations, including those that are glycinergic, glutamatergic, and nitric oxide positive (Chan and Sawchenko, 1998), barosensitive NTS neurons have been shown to be primarily glutamatergic (Sapru, 2002; Suzuki et al., 1996).

Interestingly, the NTS also contains a population of non-barosensitive GABAergic neurons which project onto the barosensitive, excitatory NTS cells. The inputs to such inhibitory NTS interneurons to date are not well characterized, yet some believe they may receive inputs from rostral nuclei including the mesencephalic locomotor region and the hypothalamus (Degtyarenko and Kaufman, 2005). Chen et al. (2009) have also indicated that this population of GABAergic neurons receives inputs from muscle afferents and that following exercise they contribute to the phenomenon of post-exercise hypotension. In addition, Tsukamoto and Sved (1993) have reported that microinjection of a $GABA_B$ receptor antagonist into the NTS leads to a significant drop in blood pressure. This suggests that although the main phenotype of the barosensitive neuron within the NTS is glutamatergic, GABA secretion from NTS interneurons appears to play an important role in the regulation of blood pressure through inhibition of glutamatergic NTS efferents.

From the NTS the signal is relayed to the CVLM (Gordon & Sved, 2002; Kawai & Emiko, 2000). Because of its robust collection of GABAergic cell bodies, the CVLM has been termed the 'depressor region.' For instance, Agrawal et al. (1989) demonstrated that excitation of the CVLM with L-glutamate microinjections leads to marked decreases in mean arterial pressure, MAP. Conversely, inhibition of the CVLM cells via administration of the $GABA_A$ receptor agonist muscimol leads to significant increases in MAP (Willette et al., 1984), and as expected, destruction of the CVLM leads to drastic increases in MAP (Imaizumi, 1985).

The inhibitory, GABAergic efferents of the CVLM project to the RVLM (Chan & Sawchenko, 1998; Minson et al., 1997), and their functional importance has been documented by microinjections of the $GABA_A$ agonist muscimol into the RVLM, which cause large decreases in MAP (Schreihofer et al., 2000). The RVLM contains glutamatergic cells that project down the spinal cord, modulating end organ function. For example, electrical and pharmacological activation of the RVLM cell bodies results in large increases in MAP, while its bilateral destruction leads to a drop in MAP equivalent to that observed in spinalized animals (Ross et al., 1984). These studies, along with evidence of glutamatergic RVLM projections to the intermediolateral cell column (Matsumoto et al., 1994), bolster the current notion of the RVLM as a source of excitatory drive to sympathetic vasomotor efferents.

While activity of RVLM neurons is under tonic suppression from the CVLM, the source of its excitatory inputs remains to be elucidated. To answer this question, Guyenet and colleagues (1987) blocked excitatory amino acid (EAA) receptors within the RVLM with EAA receptor antagonists. This resulted in no overall change in MAP. More recently, Kiely and Gordon (1994) and Horiuchi et al. (2004) report the same phenomenon. At the current time no excitatory inputs to the RVLM have been reported except for sparse projections from the NTS (Ross et al., 1985). Such claims have been dismissed by electrophysiological (Agarwal & Calaresu, 1991) and pharmacological (Blessing, 1988) evidence of an NTS-CVLM-RVLM pathway (Chan & Sawchenko, 1998). As a result of this, some have attributed the RVLM's firing to intrinsic, pulse-mediated auto-activity (Horiuchi et al., 2004).

In summary, excitatory afferent signals originating at baroreceptors within the carotid sinus and aortic arch synapse onto NTS neurons. The NTS also receives input from more rostral nuclei. These rostral projections appear to synapse on GABAergic, inhibitory NTS interneurons. Once integration within the NTS has taken place, its excitatory, glutamatergic cell population projects to the CVLM. The CVLM relays the signal via its inhibitory GABAergic projections to the RVLM. From the RVLM the signal is sent down the spinal cord toward the target vasculature (Fig. 2).

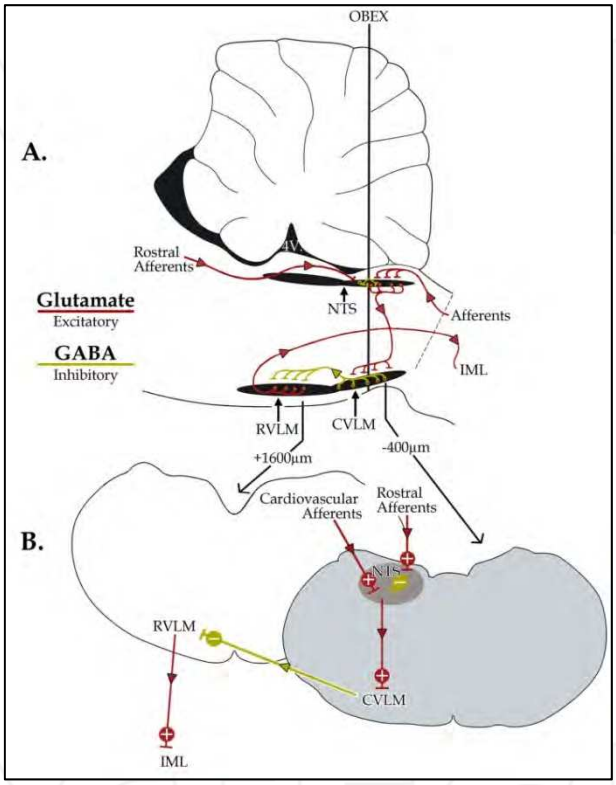

Fig. 2. Central cardiovascular circuitry. (A) Sagittal brainstem section showing the main regions involved in cardiovascular regulation. Baroreceptor afferents terminate within the NTS, which sends projections to CVLM, which in turn sends GABAergic projections to RVLM. (B) Coronal brainstem sections at +1,600 µm and -400 µm relative to the obex. Abbreviations: CVLM, caudal ventrolateral medulla; NTS, nucleus of the solitary tract; RVLM rostral ventrolateral medulla; VMM, ventromedial medulla; MLR, mesencephalic locomotor region; 4V, fourth ventricle; IML, intermediolateral cell column.

1.4 Concluding introductory remarks

Central cardiovascular control regions within the high and low aerobic capacity strains of rat used in this study are yet to be characterized. The objectives of the present study are: (1) to characterize the expression of both *Gad65* and *Gad67* within the NTS and VLM nuclei of

high and low aerobic capacity rats; and (2) to propose a neural mechanism underlying hypertension within the LCR phenotype.

2. Materials and methods

All procedures conducted were approved by the University Committee on the Use and Care of Animals at the University of Michigan and adhered to the outlines described in the Guide for the Care and Use of Laboratory Animals (National Academy of Sciences, 1996).

2.1 Rat strain

The HCR and LCR phenotypes were developed as described by Koch and Britton (2001). Briefly, 96 male and 96 genetically heterogeneous female rats were obtained from the N:NIH stock at the National Institutes of Health (Bethesda, MD). At 10 weeks of age all rats were given treadmill education for a period of 1 week. Education consisted of familiarizing the rats to the treadmill and the mild shock stimulus (1.2 mA at 3 Hz for ~1.5 s) given when they traveled off the back of the treadmill. Once the rats learned to run in avoidance of the stimulus they were tested. In the event a rat did not become acclimated to the treadmill after the prescribed education period, it was not further tested and was excluded from the study.

The following week, at the age of 12 weeks, those rats which reached threshold were tested on 5 consecutive days. Using their single best day the rats were sorted, and the 13 highest and 13 lowest capacity rats for each sex were randomly paired within their newly acquired phenotype for breeding. The offspring from these pairs were weaned 28 days after birth and began treadmill education at the age of 10 weeks, at which time the process, as stated above, was repeated. In following generations (F1 onward), the only deviation from the above protocol was that no minimum threshold was required for inclusion in the study. Additionally, it should be noted that after initiation of the F1 generation from the founder population, all subsequent generations were bred using within-family rotational breeding methods between the original 13 families for each phenotype in order to minimize inbreeding.

2.2 Tissue collection and sectioning

8 adult HCR and 8 adult LCR male rats were obtained from the 18th generation. Animals were housed in pairs, with each cage containing a pair of either HCR or LCR male rats. Food and water were readily available to all animals, and cages were kept in a 12 hour light, 12 hour dark environment.

Rats were sacrificed via rapid decapitation using a guillotine. The brains were extracted, flash frozen in 2-methylbutane at -30˚C, and stored at -80˚C until further processing took place. At the time of sectioning each brain was removed from -80˚C and allowed to equilibrate at -20˚C within the cryostat for 5 minutes. At this time each brain was dissected in two at the level of the anterior thalamus to allow for mounting of the tissue on a block. The caudal half of the dissected tissue was mounted and subsequently embedded with M-1 embedding matrix (Thermo Shandon, Pittsburgh, PA). The tissue was then sectioned on a cryostat (Leica CM1850) at -20˚C at a thickness of 10µm in the coronal plane throughout the entire rostro-caudal extent of the medulla. Sections were mounted 4 per slide on Superfrost

slides (Fischer Scientific) by apposing the slides kept at room temperature onto the cryostat stage. A total of 100 slides were taken per animal, resulting in a total sectioned distance of 4.0 mm. Following sectioning, slides were stored at -80˚C until further processing.

2.3 Tissue mapping

To standardize tissue levels between animals, every tenth slide was pulled from storage and allowed to equilibrate at room temperature for ~2 minutes. Slides were then stained for 5 minutes in a 1% cresyl violet solution containing 1% glacial acetic acid. Following the 5 minute incubation, sections were placed in water for 30 seconds and then dehydrated as follows: 30 seconds each in 50% ethanol, 70% ethanol, 85% ethanol, 95% ethanol (twice), and 100% ethanol (twice). Following the final 100% ethanol wash, slides were placed in xylene for at least 5 minutes and pulled to be coverslipped with Permount (Fischer Scientific) and standard laboratory coverglass.

Following a 2 day drying period slides were examined under a microscope. The obex, which we classify as the opening of the 4th ventricle, was located and recorded for all brains. By using these reference slides we were able to align all brains relatiave to each other and in relation to the obex (Fig. 3).

2.4 *In situ* hybridization

Gene expression of *Gad65* and *Gad67* was quantified using radioactive *in situ* hybridization. Total rat brain RNA was obtained, reverse-transcribed, and then subjected to the polymerase chain reaction (PCR) to amplify *Gad65* and *Gad67* mRNA. *Gad* PCR products were then purified via agarose gel electrophoresis. Representative bands were excised, and the resulting RNA was purified. Purified RNA was then subcloned into Bluescript SK vectors containing both T3 and T7 promoter sequences (Stratagene, San Diego, CA). Vectors were introduced into *E. Coli* bacteria and stored at -80˚C in a 50% glycerol stock until further processing.

Prior to the execution of the below experiments, plasmid DNA containing the *Gad* insert was extracted from bacteria clones and sequenced. Sequencing results obtained by automated deoxynucleotide sequencing at the University of Michigan DNA sequencing core matched those provided by NCBI's local alignment search tool (BLAST) available at www.ncbi.nlm.nih.gov/BLAST/.

Radioactive probe manufacturing: E. Coli containing Bluescript vectors with the *Gad65* or *Gad67* insert were removed from -80˚C storage and grown at 37˚C for 16 hours in a shaker set to 250 rpms. Following the 16 hour incubation the bacterial clones were removed from the shaker and centrifuged at 7000 rpms in a Beckman centrifuge (SM-24 rotor) for 10 minutes. The less dense supernatant was poured off, and the plasmids were extracted and purified using a Qiagen QIAprep Spin Miniprep Kit (Qiagen, Hilden, Germany). "The bench protocol: QIAprep Spin Minipred Kit using a microcentrifuge" protocol was follow precisely except for the last step, where 40µl of Buffer EB was used to elute DNA rather than 50µl.

At this time a reaction to "pop-out" the insert was conducted to ensure the insert was of the expected size – 640 nt for *Gad65* (NCBI accession number: M72422) and 900 nt for *Gad67* (NCBI accession number: M34445). 2µl of the eluted DNA was added to 14µl of distilled

water, 2µl of 10x React3 buffer (Invitrogen, Carlsbad, CA), 1µl of EcoR1 enzyme (Invitrogen, 10U/µl), and 1µl of BamH1 enzyme (Invitrogen, 10units/µl). The mix was incubated at 37˚C for 1 hour. Simultaneously, 20µl of the eluted DNA was linearized by adding 10µl of 10x React2 buffer (for anti-sense; Invitrogen) or 10x React3 buffer (Sense), 50µl of distilled water, and 5µl of Hind3 (Anti-Sense; Invitrogen, 10units/µl) or BamH1 (Sense; Invitrogen, 10uU/µl). This mixture was incubated at 37˚C for 2 hours. Following the incubations the products were run out on a 2% agarose gel and visualized using ethidium bromide.

Sense and anti-sense cRNA probes were synthesized as follows: 4µl ^{35}S-UTP (10µCi/µl; Amersham Biosciences, Piscataway, NJ) and 3µl ^{35}S-CTP (10µCi/µl; Amersham Biosciences) were added to 5µl of 5x T3/T7 buffer (Invitrogen), 5µl of filtered water, 1µl ATP (10mM), 1µl GTP (10mM), 1µl RNAse inhibitor (40U/µl; GeneChoice, Frederick, MD), 2µl 0.1M DTT (Invitrogen), 2µl of linearized DNA, and 1µl of T3 polymerase (40units/µl; Invitrogen). The contents were allowed to incubate in a water bath set to 37˚C for 2 hours. Following the 2 hour incubation, 1µl of RNAse-free DNAse (10U/µl; Roche Scientific, Basel, Switzerland) was added, and the mixture was allowed to sit at room temperature for 15 minutes, after which the contents were transferred to a drained BioRad Micro Bio-Spin Chromatography column (BioRad, Hercules, CA). The manufacturer's protocol was followed except for the last step. Briefly, the column was allowed to drain for 5 minutes followed by a 2 minute 1000g spin before the probe was added. The probe was diluted with 25µl of filtered, distilled water before being added to the prepared column. The column was then placed into a clean 1.5mL eppendorf tube and spun for 4 minutes at 1000g. The column was then discarded, and 1µl of 1M DTT was added to the purified probe. At this time 1µl of the purified probe was taken, and its radioactivity was quantified using a Packard 2200CA liquid scintillation analyzer (Packard, Wellesley, MA). The remaining probe was placed at -80˚C for storage (< 3 days).

Preparation of the tissue: Slides were removed from storage at -80˚C and placed in 4% paraformaldehyde at room temperature for 1 hour. They were then transferred to 2X sodium chloride/sodium citrate solution (SSC) for 5 minutes – this step was repeated 3 times for a total of three 5 minute washes. Slides were then placed in a 0.1M triethanolamine (TEA) wash (pH = 8.0, obtained through the addition of acetic anhydride) for 10 minutes. Lastly, the slides were dehydrated by running them through a series of ethanol washes for 30 seconds each (50%, 75%, 90%, 95% twice, and 100% twice). The slides were then allowed to air dry.

Hybridization: 70µl of hybridization buffer containing 10^6 cpm of the cRNA probe and 10mM DTT was pipetted onto each slide. The slides were cover-slipped with standard cover glass and put in incubation trays containing blotting paper dampened with 50% formamide. Each tray was covered with a lid, sealed in plastic wrap, and kept at 55˚C for 18 hours.

Post-Hybridization: Following removal of coverslips, the slides were washed three times for 5 minutes in 2X SSC and were then transferred to a 37˚C RNAse A solution for 1 hour. The slides were then taken through the following washes, each of which lasted 5 minutes: 2X SSC, 1X SSC, and 0.5X SSC. A 1 hour incubation in 65-70˚C 0.1X SSC followed. Slides were then dipped in distilled water and dehydrated in ethanol (30 seconds each in 50%, 75%, 90%, 95% twice, and 100% twice).

Film/Exposure: Following dehydration, slides were allowed to dry for 15 minutes and then apposed to Kodak Biomax MR radiosensitive film. Each cassette contained alternating rows of slides with HCR or LCR tissue. Following a 72 hour exposure, cassettes were opened in the dark, and the film was developed using a Kodak X-OMAT 2000A processor (Eastman Kodak).

Emulsion dipping: In order to visualize individual hybridized probes, slides were emulsion dipped in K.5D emulsion gel containing silver bromide (Ilford Scientific, Cheshire, GB). Following an 11 day exposure at 10°C the slides were developed by placing them in Kodak D19 developer (Eastman Kodak, Rochester, NY) for 2 minutes, followed by 30 seconds in water, 3 minutes in Kodak Liquid Rapid Fixer Solution (Eastman Kodak, Rochester, NY), 30 seconds in water to wash off the fixer, and 15 minutes under cool tap water. Slides were then stained using a 1% cresyl violet solution containing 1% glacial acetic acid for 2 minutes. Slides were then briefly rinsed in water and dehydrated by taking them through a series of graded alcohols as described above (2.3 – Tissue mapping). Following the 100% ethanol washes, slides were placed in xylene for at least 5 minutes and were then pulled to be coverslipped with Permount (Fischer Scientific) and standard laboratory coverglass.

2.5 Film and image analysis

The autoradiographs were illuminated using a Northern Light Illuminator (Imaging Research, St. Catharines, ON) and then digitized with a Sony XC-ST70 video camera connected to a computer running MCID Basic software (Imaging Research, St. Catherines, ON). Images were analyzed with Scion Image Beta 4.02 software (Scion Corp., Frederick, MA) using an in-house macro designed to count only those pixels which were 3.5 standard deviations above the average background value. Background was calculated for each image using an area of tissue containing no *Gad* expression such as white matter tracts. Signal and integrated optical density (IOD) values for each nucleus of interest within each section were calculated. IOD is defined as the area of highlighted pixels multiplied by the average density (i.e. signal) of each pixel, expressed in arbitrary units. Signal and IOD measurements were averaged between left and right sides. Each region of interest was analyzed across multiple rostro-caudal levels that were matched between HCR and LCR samples.

For illustration purposes, emulsion dipped slides were digitized using a Sony DXC 970MD color video camera (Sony Corp.) connected to a Leica DMRD microscope (Leica, Wetzlar, Germany). All equipment was connected to a computer running MCID Basic (Imaging Research).

2.6 Data analysis

Statistical analyses were performed using SPSS version 13 software (SPSS Inc., Chicago, IL). To assess for differences between the HCR and LCR phenotypes at various caudal-to-rostral levels, linear mixed effects model statistics were conducted. Within the model, repeated covariance types were selected based on Akaike's information criterion (AIC). In all cases, heterogeneous first-order autoregressive (ARH1) produced the smallest AIC value and was thus used for all analyses. In the event the model reached significance, post-hoc testing was conducted. P-values for multiple t-tests were corrected for using Bonferroni correction. Significance was set to $p<0.05$ in all cases. Data are presented as mean ± SEM.

3. Results

Our initial analysis focused on the distribution of *Gad65* and *Gad67* mRNA in the medulla of HCR and LCR rats. Labeling for *Gad65* and *Gad67* was present throughout the brainstem and included VLM, ventromedial medulla, NTS, area postrema, raphe nuclei, vestibular

nuclei, and spinal trigeminal nucleus (Fig. 3). Labeling was absent in motor nuclei, such as the facial nerve nucleus and the hypoglossal nerve nucleus. Examination of emulsion dipped material revealed dense clustering of grains over cresyl violet stained nuclei within the same locations as revealed by the radiographs, including NTS (Fig. 4). The general patterns of *Gad65* and *Gad67* mRNA distributions were very similar.

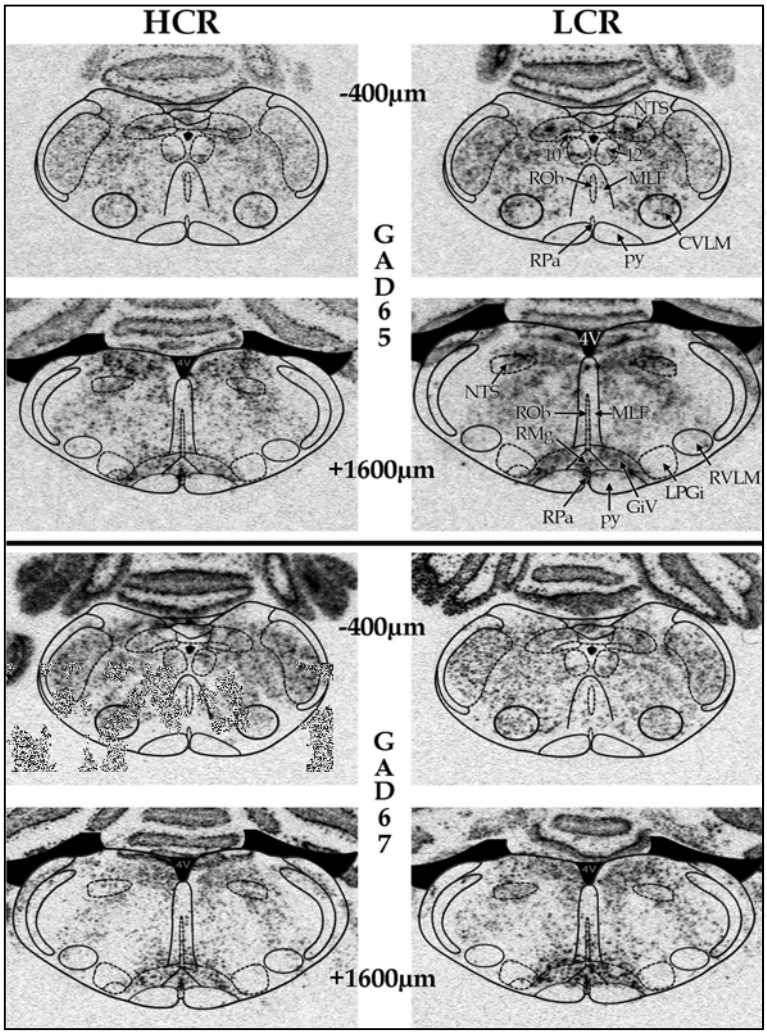

Fig. 3. Autoradiographs illustrating *Gad65* (top) and *Gad67* (bottom) expression at -400 µm and +1,600 µm relative to obex. Abbreviations: 10 – dorsal motor nucleus of the vagus; 12 – hypoglossal nerve nucleus; CVLM, caudal ventrolateral medulla; GiV, ventral gigantocellular nucleus; MLF – medial longitudinal fasciculus; LPGi, lateral paragigantocellular nucleus; py, pyramidal tract; RMg, raphe magnus; ROb, raphe obscurus, RPa, raphe pallidus; RVLM, rostral ventrolateral medulla.

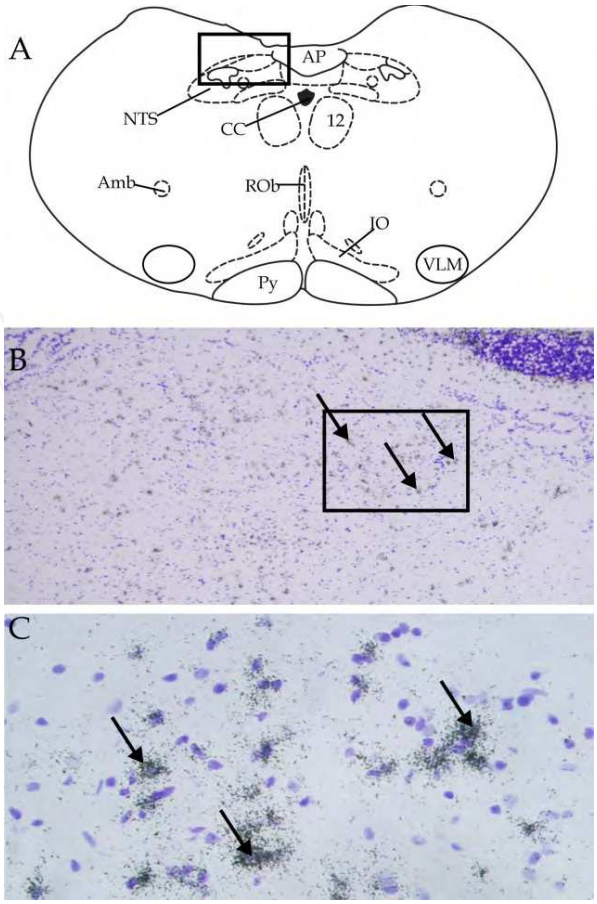

Fig. 4. Emulsion dipped material revealed dense clusters of dark grains corresponding to *Gad65* mRNA. (A) Drawing of the brainstem at -400 μm relative to obex, adapted from the atlas of Paxinos and Watson. (B) 5x image of NTS (see boxed area in 5A). Arrows indicate examples of dense GAD65 expression. (C) 63x image of boxed area in figure 5B. Slides were counter-stained with cresyl violet (purple) to highlight cell nuclei. Again arrows indicate dense grain clusters, corresponding to GABAergic neurons. Abbreviations: Amb, nucleus ambiguus; AP, area postrema; CC, central canal; IO, inferior olive; NTS, nucleus of the solitary tract; Py, pyramidal tract; ROb, raphe obscurus; VLM, ventrolateral medulla.

The expression of *Gad65* mRNA in LCR and HCR rats was quantified within NTS and VLM. Significant main effects of level and phenotype were observed within both regions ($p < 0.05$), indicating that LCR rats had higher levels of *Gad65* mRNA compared to HCR rats.

Analysis of the signal data revealed an upregulation in *Gad65* expression in LCR animals within the caudal NTS at -400 μm relative to the obex (Fig. 5A). We observed a similar upregulation in *Gad65* expression in the VLM of LCR rats both caudally (at -400 μm) and rostrally (at +400 μm and +1200 μm; Fig. 5B).

Analysis of the IOD data confirmed these observations and revealed increased *Gad65* expression in LCR animals at -800 µm and -400 µm in the NTS (Fig. 5C), as well as at +400 µm within the VLM (Fig. 5D).

In the case of *Gad67* mRNA, no significant differences in its expression were detected between HCR and LCR rats in either NTS or VLM.

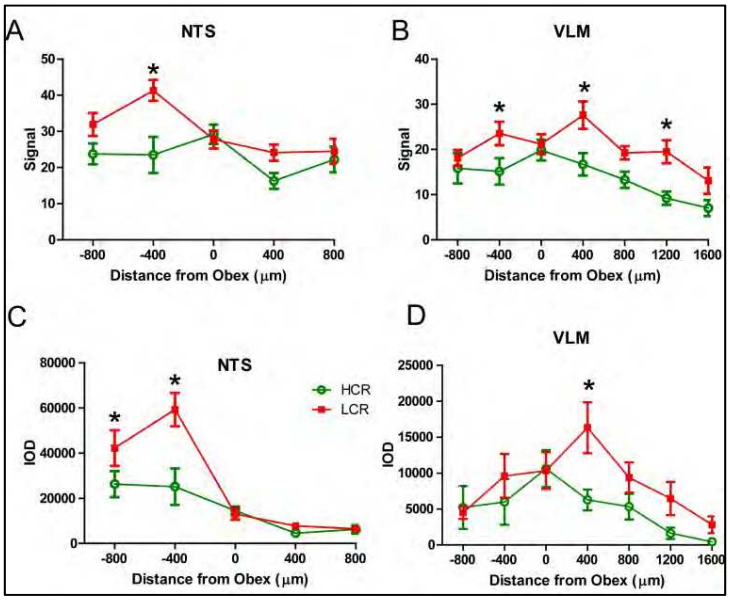

Fig. 5. Upregulation of *Gad65* expression within NTS and VLM in LCR rats. Note increase in expression at specific rostro-caudal levels. * - $p < 0.05$ compared to HCR. Adapted from Buck et al., 2007.

4. Discussion

The current study quantified expression of the GABA synthesizing enzymes *Gad65* and *Gad67* in the brainstem of a rat model of MetS (i.e. LCR) as compared to its high aerobic capacity counterpart (i.e. HCR rat). As described previously, the low capacity running rats, LCRs, exhibited dramatically poorer exercise capacity compared to their high capacity, HCR, counterparts. LCR rats became exhausted more quickly, ran for a shorter distance, and ran at a slower pace compared to HCR rats. The LCR animals also weighed significantly more than their HCR counterparts (Buck et al., 2007), and previous characterization demonstrates elevated mean blood pressures in the LCR strain equating to a roughly 13 mmHg difference (Wisloff et al., 2005). These findings together with prior observations of increased visceral adiposity and increased insulin resistance suggest that LCR animals may represent an animal model of metabolic syndrome (Wisloff et al., 2005).

Specifically, this study examined the distribution of *Gad65* and *Gad67* in baro-responsive nuclei in the brainstems of both the HCR and LCR phenotypes. Our hypothesis was that alterations in brainstem circuitry, specifically involving the inhibitory neurotransmitter

GABA, contribute to the observed variations in mean arterial pressure between the two groups.

4.1 Nucleus of the solitary tract, NTS

GABA containing neurons within the NTS were first described by Chan and Sawchenko (1998), who identified a small population of baro-sensitive GABAergic neurons within the NTS. More recently, however, Degtyarenko and Kaufman (2005) demonstrated a larger collection of non-barosensitive GAD- containing interneurons within the NTS. Significantly outnumbering the small population of baro-sensitive neurons, this newly characterized population likely exerts far more influence on the cardiovascular circuitry (Degtyarenko and Kaufman, 2005). It should be noted, however, that inputs to these NTS interneurons are still mostly undocumented, although some believe they receive their input from the mesencephalic locomotor region and are integral in resetting the circuitry during exercise (Degtyarenko and Kaufman, 2005). Other reports have indicated that this population receives inputs from muscle afferents (Chen et al., 2009), and that following exercise they contribute to the phenomenon of post-exercise hypotension. Full characterization of inputs to GAD containing NTS cells, however, is yet to be determined.

The present study set out to determine differences in expression of both *Gad65* and *Gad67* in the NTS of HCR and LCR rats. Our data suggest that increased levels of *Gad65* may lead to increased levels of GAD65 protein, which would result in increased synthesis of GABA within the caudal NTS. It seems likely that these changes predominantly impact inhibitory interneurons within the NTS. Such interneurons play a critical role in regulating excitatory output from the NTS and may contribute to elevated arterial pressure in the LCR rats through inhibition of excitatory influence on the CVLM.

No differences were seen in *Gad67* expression between the HCRs and LCRs. However, GAD67 is likely responsible for long-term maintenance of cytoplasmic pools of GABA and is used to set baseline levels (Esclapez et al., 1994; Soghomonian & Martin, 1998; Esclapez & Houser, 1999). GAD65, on the other hand, regulates local control of GABA synthesis and represents vesicular synthesis (Soghomonian & Martin, 1998), thus playing a prominent role in GABAergic neurotransmission.

4.2 Ventrolateral medulla, VLM

Past research involving microinjections of excitatory and inhibitory transmitters into the VLM led to the identification of physiologically defined pressor and depressor regions, respectively (Schreihofer & Guyenet, 2002). Schreihofer and Guyenet went on to map these two regions relative to the obex in the adult rat. Their experimentation resulted in a CLVM depressor region extending from -500μm to +1000μm relative to the obex and a RVLM pressor region extending from +700μm to +2000μm, ending at the caudal pole of the facial nerve nucleus.

In the present study we observed an upregulation in the expression of *Gad65* mRNA in both the rostral and caudal VLM in LCR rats. While upregulation of *Gad65* within the CVLM may be a compensatory response to chronic elevation in blood pressure, the findings in the RVLM do not fit the currently accepted model of central control of vascular tone. According to the classical model, increased GABAergic neurotransmission within the rostral VLM would lead to lower, not higher, blood pressure, as we observed in the LCR rats (Guyenet,

2006). Though the latter finding is difficult to resolve with existing literature, there may be other possibilities that may explain this observation. One option is that this alteration in *Gad65* mRNA expression occurs in non-cardiovascular neurons. Rostral VLM is a heterogeneous region that also contains neurons with respiratory functions (Richter & Spyer, 2001). Thus, up-regulation in expression of *Gad65* mRNA in the rostral VLM of LCR rats may represent potential alterations in respiratory function.

Another possibility is that the presumed increase in GABAergic neurotransmission activates an "accessory" vasomotor pathway originating from the rostral VLM (McAllen et al., 2005). This pathway is thought to activate "accessory" sympathetic preganglionic neurons, which are characterized by their unmyelinated axons and which drive hexamethonium-resistant transmission in sympathetic ganglia (McAllen et al., 2005). Unlike "regular" sympathetic preganglionic neurons, which are inhibited by administration of GABA in the rostral VLM, the "accessory" sympathetic preganglionic neurons are activated by this manipulation (McAllen et al., 2005). Thus, it may be that activation of this "accessory" pathway contributes to resting blood pressure differences between LCR and HCR rats.

Yet another possibility is that increased *Gad65* mRNA expression in the rostral VLM of LCR rats leads to increased GABA production and secretion within projection neurons, rather than local interneurons. Data from anatomical and pharmacological experiments suggest that neurons within the rostral VLM project to the NTS, where they inhibit the baroreceptor reflex (Len & Chan, 2001; Livingston & Berger, 1989; Loewy et al., 1981). This notion is supported by the observation that administration of glutamate into the rostral VLM, but not into surrounding regions, leads to the release of GABA in the caudal NTS (Len & Chan, 2001). This glutamate-induced increase in GABA secretion in the NTS is associated with the suppression of the baroreceptor reflex, an effect that is blocked by administration of $GABA_A$ and $GABA_B$ receptor antagonists in the NTS (Len & Chan, 2001). Such an increase in baroreflex inhibition would lead to higher resting blood pressure levels, which may contribute to increased blood pressure levels in LCR rats. Future studies will be required to test these hypotheses.

5. Conclusions and future directions

The present study examined potential differences in the expression of *Gad65* and *Gad67* mRNA within brainstem cardiovascular control nuclei in a rat model of metabolic syndrome. Our goal was to assess for differences in GABAergic tone as an explanation for hypertension in the LCR phenotype. We found increased levels of *Gad65*, but not *Gad67*, expression within the caudal NTS, caudal VLM, and rostral VLM of LCR rats compared to their HCR counterparts. These findings suggest a neural component in the development of hypertension in MetS.

To better understand brainstem contributions in the development of hypertension in MetS, further studies are needed to more fully characterize inputs to GABAergic NTS neurons. Additionally, past studies have highlighted an up-regulation of $GABA_B$ receptor mRNA in the NTS of hypertensive rats (Durgam et al., 1999). $GABA_B$ receptor expression appears to be important in mediating increases in MAP during rest (Tolstykh et al., 2003). Thus, examination of potential $GABA_B$ receptor expression and function differences between HCR and LCR rats may add additional insight into the pathophysiology of hypertension associated with MetS.

6. Acknowledgements

The authors would like to thank Dr. Stanley Watson who allowed us to conduct much of this work in his laboratory at the University of Michigan. We are grateful to Sharon Burke and Jennifer Fitzpatrick for their technical assistance. Without them this chapter would not have been possible. Additionally we acknowledge Huda Akil, Ph.D. for her support of the project, as well as Dr. Paul Burghardt and Dr. Sarah Clinton for sharing their knowledge of *in situ* hybridization and radiographic quantification. Supported by: 4R00MH081927-03 (IAK).

7. References

Agarwal SK, Calaresu FR (1991) Monosynaptic connection from caudal to rostral ventrolateral medulla in the baroreceptor reflex pathway. Brain Res 555:70-74.

Agarwal SK, Gelsema AJ, Calaresu FR (1989) Neurons in rostral VLM are inhibited by chemical stimulation of caudal VLM in rats. Am J Physiol 257:R265-270.

Alberti KG, Zimmet P, Shaw J (2005) The metabolic syndrome--a new worldwide definition. Lancet 366:1059-1062.

Altschuler SM, Bao XM, Bieger D, Hopkins DA, Miselis RR (1989) Viscerotopic representation of the upper alimentary tract in the rat: sensory ganglia and nuclei of the solitary and spinal trigeminal tracts. J Comp Neurol 283:248-268.

Andresen MC, Doyle MW, Jin YH, Bailey TW (2001) Cellular mechanisms of baroreceptor integration at the nucleus tractus solitarius. Ann N Y Acad Sci 940:132-141.

Blessing WW (1988) Depressor neurons in rabbit caudal medulla act via GABA receptors in rostral medulla. Am J Physiol 254:H686-692.

Blessing WW, Nalivaiko E (2001) Raphe magnus/pallidus neurons regulate tail but not mesenteric arterial blood flow in rats. Neuroscience 105:923-929.

Buck BJ, Kerman IA, Burghardt PR, Koch LG, Britton SL, Akil H, Watson SJ (2007) Upregulation of GAD65 mRNA in the medulla of the rat model of metabolic syndrome. Neurosci Lett 419:178-183.

Chan RK, Sawchenko PE (1994) Spatially and temporally differentiated patterns of c-fos expression in brainstem catecholaminergic cell groups induced by cardiovascular challenges in the rat. J Comp Neurol 348:433-460.

Chan RK, Sawchenko PE (1998) Organization and transmitter specificity of medullary neurons activated by sustained hypertension: implications for understanding baroreceptor reflex circuitry. J Neurosci 18:371-387.

Chen CY, Bechtold AG, Tabor J, Bonham AC (2009) Exercise reduces GABA synaptic input onto NTS baroreceptor second-order neurons via NK1 receptor internalization in spontaneously hypertensive rats. J Neurosci 29(9):2754-2761.

Chua SC, Chung WK, Wu-Peng XS, Zhang Y, Liu SM, Tartaglia L, Leibel RL (1996) Phenotypes of mouse *diabetes* and rat *fatty* due to mutations in the OB (leptin) receptor. Science 271(5251):994-996.

d'Ascanio P, Centini C, Pompeiano M, Pompeiano O, Balaban E (2002) Fos and FRA protein expression in rat nucleus paragigantocellularis lateralis during different space flight conditions. Brain Res Bull 59:65-74.

Dampney RA (1994) The subretrofacial vasomotor nucleus: anatomical, chemical and pharmacological properties and role in cardiovascular regulation. Prog Neurobiol 42:197-227.

Danbolt NC (2001) Glutamate uptake. Prog Neurobiol 65:1-105.

de Artinano AA, Castro MM (2009) Experimental rat models to study the metabolic syndrome. British Journal of Nutrition 102:1246-1253.

Degtyarenko AM, Kaufman MP (2005) MLR-induced inhibition of barosensory cells in the NTS. Am J Physiol Heart Circ Physiol 289:H2575-2584.

Devaney JM, Gordish-Dressman H, Harmon BT, Bradbury MK, Devaney SA, Harris TB, Thompson PD, Clarkson PM, Price TB, Angelopoulos TJ, Gordon PM, Moyna NM, et al. (2011) *AKT1* polymorphisms are associated with risk for metabolic syndrome. Hum Genet 129:129-139.

Durgam VR, Vitela M, Mifflin SW (1999) Enhanced gamma-aminobutyric acid-B receptor agonist responses and mRNA within the nucleus of the solitary tract in hypertension. Hypertension 33:530-536.

Erickson JT, Millhorn DE (1991) Fos-like protein is induced in neurons of the medulla oblongata after stimulation of the carotid sinus nerve in awake and anesthetized rats. Brain Res 567:11-24.

Esclapez M, Tillakaratne NJ, Kaufman DL, Tobin AJ, Houser CR (1994) Comparative localization of two forms of glutamic acid decarboxylase and their mRNAs in rat brain supports the concept of functional differences between the forms. J Neurosci 14:1834-1855.

Esclapez M, Houser CR (1999) Up-regulation of GAD65 and GAD67 in remaining hippocampal GABA neurons in a model of temporal lobe epilepsy. J Comp Neurol 412:488-505.

Fong AY, Stornetta RL, Foley CM, Potts JT (2005) Immunohistochemical localization of GAD67-expressing neurons and processes in the rat brainstem: subregional distribution in the nucleus tractus solitarius. J Comp Neurol 493:274-290.

Ford ES, Giles WH, Dietz WH (2002) Prevalence of the metabolic syndrome among US adults: findings from the third National Health and Nutrition Examination Survey. Jama 287:356-359.

Gordon FJ, Sved AF (2002) Neurotransmitters in central cardiovascular regulation: glutamate and GABA. Clin Exp Pharmacol Physiol 29:522-524.

Graham JC, Hoffman GE, Sved AF (1995) c-Fos expression in brain in response to hypotension and hypertension in conscious rats. J Auton Nerv Syst 55:92-104.

Grisk O, Frauendorf T, Schluter T, Kloting I, Kuttler B, Krebs A, Ludemann J, Rettig R (2007) Impaired coronary function in Wistar Ottawa Karlsburg W rats--a new model of the metabolic syndrome. Eur J Physiol 454:1011-1021.

Grundy SM, Brewer HB, Jr., Cleeman JI, Smith SC, Jr., Lenfant C (2004) Definition of metabolic syndrome: Report of the National Heart, Lung, and Blood Institute/American Heart Association conference on scientific issues related to definition. Circulation 109:433-438.

Guyenet PG, Filtz TM, Donaldson SR (1987) Role of excitatory amino acids in rat vagal and sympathetic baroreflexes. Brain Res 407:272-284.

Guyenet PG (2006) The sympathetic control of blood pressure. Nat. Rev. Neurosci. 7: 335–346.

Hermann GE, Bresnahan JC, Holmes GM, Rogers RC, Beattie MS (1998) Descending projections from the nucleus raphe obscurus to pudendal motoneurons in the male rat. J Comp Neurol 397:458-474.

Hisano S (2003) Vesicular glutamate transporters in the brain. Anat Sci Int 78:191-204.

Horiuchi J, Killinger S, Dampney RA (2004) Contribution to sympathetic vasomotor tone of tonic glutamatergic inputs to neurons in the RVLM. Am J Physiol Regul Integr Comp Physiol 287:R1335-1343.

Imaizumi T, Granata AR, Benarroch EE, Sved AF, Reis DJ (1985) Contributions of arginine vasopressin and the sympathetic nervous system to fulminating hypertension after destruction of neurons of caudal ventrolateral medulla in the rat. J Hypertens 3:491-501.

Ishizuka T, Ernsberger P, Liu S, Bedol D, Lehman TM, Koletsky RJ, Friedman JE (1998) Phenotypic consequences of a nonsense mutation in the leptin receptor gene (fak) in obese spontaneously hypertensive Koletsky rats (SHROB). J Nutr 128(12):2299-306.

Len WB, Chan JY (2001) Rostralventrolateralmedullasuppressesreflexbradycardia by the release of gamma-aminobutyric acid in nucleus tractus solitarii of the rat. Synapse 39: 23–31.

Kandler K, Herbert H (1991) Auditory projections from the cochlear nucleus to pontine and mesencephalic reticular nuclei in the rat. Brain Res 562:230-242.

Kang TC, Kim HS, Seo MO, Choi SY, Kwon OS, Baek NI, Lee HY, Won MH (2001) The temporal alteration of GAD67/GAD65 ratio in the gerbil hippocampal complex following seizure. Brain Res 920:159-169.

Kawai Y, Senba E (1996) Organization of excitatory and inhibitory local networks in the caudal nucleus of tractus solitarius of rats revealed in in vitro slice preparation. J Comp Neurol 373:309-321.

Kawai Y, Senba E (2000) Electrophysiological and morphological characteristics of nucleus tractus solitarii neurons projecting to the ventrolateral medulla. Brain Res 877:374-378.

Kiely JM, Gordon FJ (1994) Role of rostral ventrolateral medulla in centrally mediated pressor responses. Am J Physiol 267:H1549-1556.

Koch LG, Britton SL (2001) Artificial selection for intrinsic aerobic endurance running capacity in rats. Physiol Genomics 5:45-52.

Korsak A, Gilbey MP (2004) Rostral ventromedial medulla and the control of cutaneous vasoconstrictor activity following i.c.v. prostaglandin E(1). Neuroscience 124:709-717.

Kovacs P, van den Brandt J, Kloting K (2000) Genetic dissection of the syndrome X in the rat. Biochemical and Biophysical Research Communications 269:660-665.

Kuo JS, Hwa Y, Chai CY (1979) Cardio-inhibitory mechanism in the gigantocellular reticular nucleus of the medulla oblongata. Brain Res 178:221-232.

Lernmark A (1996) Glutamic acid decarboxylase--gene to antigen to disease. J Intern Med 240:259-277.

Leu HB, Chung CM, Lin SJ, Jong YS, Pan WH, Chen JW (2011) Adiponectin gene polymorphism is selectively associated with the concomitant presence of metabolic syndrome and essential hypertension. PLoS ONE 6(5):E19999.

Livingston CA, Berger AJ (1989) Immunocytochemical localization of GABA in neurons projecting to the ventrolateral nucleus of the solitary tract. Brain Res. 494: 143–150.

Loewy AD, Wallach JH, McKellar S (1981) Efferentconnectionsoftheventral medulla oblongata in the rat. Brain Res. 228: 63–80.

Lorenzo C, Williams K, Hunt KJ, Haffner SM (2006) Trend in the prevalence of the metabolic syndrome and its impact on cardiovascular disease incidence: the San Antonio Heart Study. Diabetes Care 29:625-630.

Matsumoto M, Takayama K, Miura M (1994) Distribution of glutamate- and GABA-immunoreactive neurons projecting to the vasomotor center of the intermediolateral nucleus of the lower thoracic cord of Wistar rats: a double-labeling study. Neurosci Lett 174:165-168.

McAllen RM, Allen AM, Bratton BO (2005) A neglected 'accessory' vasomotor pathway: implications for blood pressure control. Clin. Exp. Pharmacol. Physiol. 32: 473–477.

Mei H, Chen W, Dellinger A, He J, Wang M, Yau C, Srinivasan SR, Berenson GS (2010) Principal-component-based multivariate regression for genetic association studies of metabolic syndrome components. BMC Genetics 11:100.

Minson JB, Llewellyn-Smith IJ, Chalmers JP, Pilowsky PM, Arnolda LF (1997) c-fos identifies GABA-synthesizing barosensitive neurons in caudal ventrolateral medulla. Neuroreport 8:3015-3021.

Miura M, Takayama K, Okada J (1994) Neuronal expression of Fos protein in the rat brain after baroreceptor stimulation. J Auton Nerv Syst 50:31-43.

Nakamura K, Matsumura K, Kobayashi S, Kaneko T (2005) Sympathetic premotor neurons mediating thermoregulatory functions. Neurosci Res 51:1-8.

Potts J (2006) Inhibitory neurotransmission in the nucleus tractus solitarii: implications for baroreflex resetting during exercise. Exp Physiol 91(1):59-72

Richter DW, Spyer KM (2001) Studying rhythmogenesis of breathing: comparison of in vivo and in vitro models. Trends Neurosci. 24: 464– 472.

Rizzo M, Berneis K, Corrado E, Novo S (2006) The significance of low-density-lipoproteins size in vascular diseases. Int Angiol 25:4-9.

Ross CA, Ruggiero DA, Reis DJ (1985) Projections from the nucleus tractus solitarii to the rostral ventrolateral medulla. J Comp Neurol 242:511-534.

Ross CA, Ruggiero DA, Park DH, Joh TH, Sved AF, Fernandez-Pardal J, Saavedra JM, Reis DJ (1984) Tonic vasomotor control by the rostral ventrolateral medulla: effect of electrical or chemical stimulation of the area containing C1 adrenaline neurons on arterial pressure, heart rate, and plasma catecholamines and vasopressin. J Neurosci 4:474-494.

Ruggiero DA, Cravo SL, Golanov E, Gomez R, Anwar M, Reis DJ (1994) Adrenergic and non-adrenergic spinal projections of a cardiovascular-active pressor area of medulla oblongata: quantitative topographic analysis. Brain Res 663:107-120.

Sapru HN (2002) Glutamate circuits in selected medullo-spinal areas regulating cardiovascular function. Clin Exp Pharmacol Physiol 29:491-496.

Schreihofer AM, Guyenet PG (2002) The baroreflex and beyond: control of sympathetic vasomotor tone by GABAergic neurons in the ventrolateral medulla. Clin Exp Pharmacol Physiol 29:514-521.

Schreihofer AM, Stornetta RL, Guyenet PG (2000) Regulation of sympathetic tone and arterial pressure by rostral ventrolateral medulla after depletion of C1 cells in rat. J Physiol 529 Pt 1:221-236.

Seiders EP, Stuesse SL (1984) A horseradish peroxidase investigation of carotid sinus nerve components in the rat. Neurosci Lett 46:13-18.

Silva NF, Pires JG, Dantas MA, Futuro Neto HA (2002) Excitatory amino acid receptor blockade within the caudal pressor area and rostral ventrolateral medulla alters cardiovascular responses to nucleus raphe obscurus stimulation in rats. Braz J Med Biol Res 35:1237-1245.

Soghomonian JJ, Martin DL (1998) Two isoforms of glutamate decarboxylase: why? Trends Pharmacol Sci 19:500-505.

Spyer KM (1994) Annual review prize lecture. Central nervous mechanisms contributing to cardiovascular control. J Physiol 474:1-19.

Stornetta RL, McQuiston TJ, Guyenet PG (2004) GABAergic and glycinergic presympathetic neurons of rat medulla oblongata identified by retrograde transport of pseudorabies virus and in situ hybridization. J Comp Neurol 479:257-270.

Suzuki T, Takayama K, Miura M (1997) Distribution and projection of the medullary cardiovascular control neurons containing glutamate, glutamic acid decarboxylase, tyrosine hydroxylase and phenylethanolamine N-methyltransferase in rats. Neurosci Res 27:9-19.

Sved AF, Tsukamoto K (1992) Tonic stimulation of GABAB receptors in the nucleus tractus solitarius modulates the baroreceptor reflex. Brain Res 592:37-43.

Talman WT, Perrone MH, Reis DJ (1980) Evidence for L-glutamate as the neurotransmitter of baroreceptor afferent nerve fibers. Science 209:813-815.

Tolstykh G, Belugin S, Tolstykh O, Mifflin S (2003) Responses to GABA(A) receptor activation are altered in NTS neurons isolated from renal-wrap hypertensive rats. Hypertension 42:732-736.

Tsukamoto K, Sved AF (1993) Enhanced gamma-aminobutyric acid-mediated responses in nucleus tractus solitarius of hypertensive rats. Hypertension 22:819-825.

Vitela M, Mifflin SW (2001) gamma-Aminobutyric acid(B) receptor-mediated responses in the nucleus tractus solitarius are altered in acute and chronic hypertension. Hypertension 37:619-622.

Willette RN, Barcas PP, Krieger AJ, Sapru HN (1983) Vasopressor and depressor areas in the rat medulla. Identification by microinjection of L-glutamate. Neuropharmacology 22:1071-1079.

Willette RN, Punnen S, Krieger AJ, Sapru HN (1984) Interdependence of rostral and caudal ventrolateral medullary areas in the control of blood pressure. Brain Res 321:169-174.

Wisloff U, Najjar SM, Ellingsen O, Haram PM, Swoap S, Al-Share Q, Fernstrom M, Rezaei K, Lee SJ, Koch LG, Britton SL (2005) Cardiovascular risk factors emerge after artificial selection for low aerobic capacity. Science 307:418-420.

Wong J, Nock NL, Xu Z, Kyle C, Daniels A, White M, Yue DK, Elston RC, Mountjoy KG (2008) J Dia Res 10:1016.

Zabenah D, Balding DJ (2010) A genome-wide association study of the metabolic sydrome in Indian Asian Men. PLoS ONE 5(8):e11961.

Zaretsky DV, Zaretskaia MV, DiMicco JA (2003) Stimulation and blockade of GABA(A) receptors in the raphe pallidus: effects on body temperature, heart rate, and blood pressure in conscious rats. Am J Physiol Regul Integr Comp Physiol 285:R110-116.

Zhou SY, Gilbey MP (1995) Sympathoexcitatory influence of a fast conducting raphe-spinal pathway in the rat. Am J Physiol 268:R1230-1235.

Zucker LM, Zucker TF (1961) Fatty, a new mutation in the rat. J Hered 52(6):275-278.

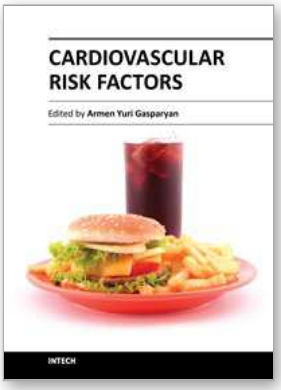

Cardiovascular Risk Factors

Edited by Prof. Armen Gasparyan

ISBN 978-953-51-0240-3
Hard cover, 498 pages
Publisher InTech
Published online 14, March, 2012
Published in print edition March, 2012

Cardiovascular risk factors contribute to the development of cardiovascular disease from early life. It is thus crucial to implement preventive strategies addressing the burden of cardiovascular disease as early as possible. A multidisciplinary approach to the risk estimation and prevention of vascular events should be adopted at each level of health care, starting from the setting of perinatology. Recent decades have been marked with major advances in this field, with the emergence of a variety of new inflammatory and immune-mediated markers of heightened cardiovascular risk in particular. The current book reflects some of the emerging concepts in cardiovascular pathophysiology and the shifting paradigm of cardiovascular risk estimation. It comprehensively covers primary and secondary preventive measures targeted at different age and gender groups. Attention is paid to inflammatory and metabolic markers of vascular damage and to the assessment of vascular function by noninvasive standardized ultrasound techniques. This is a must-read book for all health professionals and researchers tackling the issue of cardiovascular burden at individual and community level. It can also serve as a didactic source for postgraduate medical students.

How to reference

In order to correctly reference this scholarly work, feel free to copy and paste the following:

Bradley J. Buck, Lauren K. Nolen, Lauren G. Koch, Steven L. Britton and Ilan A. Kerman (2012). Alterations in the Brainstem Preautonomic Circuitry May Contribute to Hypertension Associated with Metabolic Syndrome, Cardiovascular Risk Factors, Prof. Armen Gasparyan (Ed.), ISBN: 978-953-51-0240-3, InTech, Available from: http://www.intechopen.com/books/cardiovascular-risk-factors/alterations-in-baro-sensitive-circuitry-within-the-brainstem-may-contribute-to-hypertension-in-indiv

INTECH
open science | open minds

InTech Europe
University Campus STeP Ri
Slavka Krautzeka 83/A
51000 Rijeka, Croatia
Phone: +385 (51) 770 447
Fax: +385 (51) 686 166
www.intechopen.com

InTech China
Unit 405, Office Block, Hotel Equatorial Shanghai
No.65, Yan An Road (West), Shanghai, 200040, China
中国上海市延安西路65号上海国际贵都大饭店办公楼405单元
Phone: +86-21-62489820
Fax: +86-21-62489821